

# Tutorial Problems for Nonsmooth Dynamics and Optimal Control: Ski Jumping and Accelerating a Bike Without Pedaling

Julian Golembiewski and Timm Faulwasser

**Abstract**—Nonsmooth phenomena, such as abrupt changes, impacts, and switching behaviors, frequently arise in real-world systems and present significant challenges for traditional optimal control methods, which typically assume smoothness and differentiability. These phenomena introduce numerical challenges in both simulation and optimization, highlighting the need for specialized solution methods. Although various applications and test problems have been documented in the literature, many are either overly simplified, excessively complex, or narrowly focused on specific domains. On this canvas, this paper proposes two novel tutorial problems that are both conceptually accessible and allow for further scaling of problem difficulty. The first problem features a simple ski jump model, characterized by state-dependent jumps and sliding motion on impact surfaces. This system does not involve control inputs and serves as a testbed for simulating nonsmooth dynamics. The second problem considers optimal control of a special type of bicycle model. This problem is inspired by practical techniques observed in BMX riding and mountain biking, where riders accelerate their bike without pedaling by strategically shifting their center of mass in response to the track's slope.

## I. INTRODUCTION

Many real-world control problems are characterized by nonsmooth phenomena, such as abrupt changes, impacts, switching behaviors, and nondifferentiable dynamics. These systems can generally be classified into two categories: those with internal switches, where nonsmoothness arises from state-dependent discontinuities, and those with external switches, where it is due to control-dependent discontinuities [1]. Additionally, nonsmooth systems can be further categorized based on the type of nonsmoothness they exhibit, such as continuous systems with nondifferentiable right-hand sides, systems with discontinuous dynamics, or systems with state discontinuities [2].

Established optimal control methods, which rely on smoothness and differentiability assumptions, are often insufficient for handling these complexities. This necessitates the development of specialized numerical methods to solve optimal control problems involving nonsmooth dynamics [3]. To evaluate and compare these methods, various applications and benchmark problems have been proposed in the literature.

For systems with controlled switches, a benchmark library of mixed-integer optimal control problems is provided in [4]. Other examples include a supermarket refrigeration system in [5] and a simulated moving bed chromatography system in [6]. Switched affine systems have been studied using an

abstract system model in [7]. Systems with autonomous state jumps, such as a bipedal system mimicking a walking-like motion, a bouncing ball, and a moon landing problem have been explored in [8], [9], [10]. Additionally, a benchmark library for Mathematical Programs with Complementarity Constraints (MPCCs) is given in [11].

While numerous test problems exist, many are either too abstract to be engaging for educational purposes, overly complex for testing numerical methods and prototyping, or narrowly tailored to specific application domains. In this paper, we present two novel tutorial problems in nonsmooth optimal control, combining physical intuitiveness with numerical challenges arising from their nonsmooth dynamics. These problems are introduced using basic models, with potential extensions suggested to scale complexity. First, we propose a ski jump model as an introductory problem for discretizing and simulating nonsmooth dynamical systems. Moreover, inspired by [12], [13], which use bicycle dynamics as educational example for control theory, we present a slightly different bicycle model to explore nonsmooth optimal control. The proposed Optimal Control Problem (OCP) involves nonsmooth dynamics with internal state discontinuities and sliding motion on an impact surface, a common feature in mechanical impact systems. While it seems counter-intuitive to accelerate a bike without pedaling, it is well known in mountain biking and BMX riding, that skilled riders can accelerate by shifting their body weight according to the slope of the track. On so called *pump tracks* or, e.g., in BMX Cycling at the Olympics, this is the dominant way to accelerate the bicycle.

The contribution of this paper is twofold: First, we introduce two novel tutorial problems – one serves as an entry-level example for simulating nonsmooth dynamical systems, and the other with the potential to serve as a scalable benchmark for nonsmooth optimal control. Both problems are accessible and engaging, making them well-suited for teaching purposes, while also enabling the prototyping and testing of numerical methods. We provide simulation results based on the time-freezing approach from [14] to numerically address the occurring state jumps. Second, we extend the initial investigations into modeling and optimal control of a bicycle on a pump track from [15], by explicitly incorporating jumps that result in mechanical impacts.

The remainder of this paper is organized as follows: Section II outlines the class of nonsmooth systems under consideration and presents a generic formulation of the OCP. Section III discusses numerical methods for discretizing nonsmooth dynamics and solving nonsmooth OCPs. Section IV

Julian Golembiewski and Timm Faulwasser are with the Institute of Control Systems, Hamburg University of Technology, 21079 Hamburg, Germany. E-mail: julian.golembiewski@tuhh.de, timm.faulwasser@ieee.org

introduces two tutorial problems: ski jumping and accelerating a bike without pedaling. Section V presents simulation results for these problems, and, finally, Section VI concludes the paper and suggests potential directions for future research.

*Notation:* The concatenation of two column vectors  $x \in \mathbb{R}^n$  and  $y \in \mathbb{R}^m$  is denoted by  $(x, y) := [x^\top, y^\top]^\top$ .

## II. PROBLEM SETTING AND PRELIMINARIES

### A. Class of nonsmooth dynamical systems

The problems addressed in this work involve mechanical impact systems with unilateral impact surfaces. Modeling frameworks for this class of nonsmooth dynamical systems include, but are not limited to, piecewise-smooth systems, differential inclusions, Filippov systems, dynamic complementarity systems, and Moreau's sweeping processes [16], [17], [18], [19], [20]. Studies on the optimal control of such nonsmooth systems are available, e.g., [21], [22], [23], while [24] provides a comprehensive overview with a focus on the numerical solution of nonsmooth OCPs.

In this work, we consider Nonlinear Complementarity Systems (NLCS). In this framework, the nonsmooth behavior of the dynamics is expressed as a complementarity condition. The NLCS for a mechanical impact system with unilateral impact surfaces is formulated as:

$$\dot{x} = f(x, \lambda_n, u, t) \quad (1a)$$

$$0 \leq f_c(q) \perp \lambda_n \geq 0 \quad (1b)$$

$$\text{impact laws,} \quad (1c)$$

where the state is  $x = (q, \dot{q}) \in \mathbb{R}^{n_x}$ , and  $q, \dot{q} \in \mathbb{R}^{n_q}$  are the generalized coordinates and velocities, respectively. The input is  $u \in \mathbb{R}^{n_u}$ . The impact surface is denoted by  $f_c(q)$ , and  $\lambda_n$  represents the normal contact force. The complementarity condition ensures that either (i) there is no contact force while maintaining a positive distance from the impact surface ( $\lambda_n = 0, f_c(q) > 0$ ), or (ii) a contact force exists when the distance to the impact surface is zero ( $\lambda_n > 0, f_c(q) = 0$ ).

In cases where the system undergoes state jumps due to impacts, the *impact laws* (1c) govern the associated state transitions. When the impact laws are neglected, the complementarity system defined by (1a)–(1b) can be efficiently solved using tailored methods [25]. However, in this work, we explicitly model the complexities introduced by impact laws and address them numerically using the time-freezing method outlined in [14].

### B. Optimal control formulation

Consider the continuous-time OCP

$$\min_{u(\cdot), t_f} \int_0^{t_f} \ell(t, x(t), u(t)) dt + V_f(x(t_f)) \quad (2a)$$

subject to for almost all  $t \in [0, t_f]$

$$(1), \quad x(0) = x_0 \quad (2b)$$

$$x(t) \in \mathbb{X} \subset \mathbb{R}^{n_x} \quad (2c)$$

$$u(t) \in \mathbb{U} \subset \mathbb{R}^{n_u} \quad (2d)$$

$$x(t_f) \in \mathbb{X}_f \subset \mathbb{R}^{n_x}, \quad (2e)$$

where (2b) describes a nonsmooth dynamical system with states and inputs  $x(t)$  and  $u(t)$ , respectively. This implies that the nonsmoothness may propagate state limitations, for example, through impact surfaces, leading to jump discontinuities in the velocities. Moreover, the OCP is subject to state, input, and terminal constraints. These constraints are given as compact subsets of  $\mathbb{R}^{n_x}$  and  $\mathbb{R}^{n_u}$ , respectively. The objective is to minimize the running cost  $\ell : \mathbb{R} \times \mathbb{R}^{n_x} \times \mathbb{R}^{n_u} \rightarrow \mathbb{R}_0^+$  and the terminal cost  $V_f : \mathbb{R}^{n_x} \rightarrow \mathbb{R}_0^+$  over the time horizon  $t_f \in \mathbb{R}^+$ . The terminal time  $t_f$  can also be treated as a decision variable within the OCP, enabling the formulation of free end-time problems.

## III. NONSMOOTH OPTIMAL CONTROL

Solution methods for OCPs can be broadly categorized as either indirect or direct [26]. In indirect methods, the OCP is first optimized analytically by deriving the necessary conditions of optimality using Pontryagin's Maximum Principle. These conditions are then discretized and solved numerically. In contrast, direct methods begin by discretizing the OCP itself, transforming it into a finite-dimensional nonlinear program, which is then solved numerically.

In this work, we focus on applying direct methods, which require the explicit discretization of the system dynamics. Consequently, we must address the discretization of ODEs with discontinuous right-hand sides. However, standard integration methods fail to detect switches accurately and therefore are limited to at most first-order accuracy. Additionally, the derivative information at points of discontinuity is incorrect, leading to integration errors that can accumulate over time. This can also cause the numerical solution to oscillate near discontinuities. Thus, tailored methods are required to discretize the resulting nonsmooth ODEs efficiently. Due to space limitations, we provide only a brief overview of those methods. For a more comprehensive discussion, we refer to [3], [24], [27]. For detailed analysis and convergence results, see [3], [28].

### A. Discretization of nonsmooth dynamical systems

Numerical methods for discretizing and simulating nonsmooth ODEs can be broadly categorized into event-driven schemes, time-stepping schemes, and smoothing techniques [3]. Event-driven methods focus on accurately detecting and handling discrete events where the system dynamics exhibit discontinuities. These methods define and detect events, solve the nonsmooth dynamics using reinitialization rules at the events, and perform smooth integration between events, achieving high accuracy during smooth periods. However, event-driven schemes can become inefficient when the number of events is large and are sensitive to the tolerances set for event detection.

In contrast, time-stepping methods discretize both the smooth parts of the dynamics and the complementarity conditions associated with the nonsmooth dynamics. By considering events concurrently with the integration of smooth dynamics, time-stepping schemes offer greater efficiency in scenarios with numerous events. However, they generally

provide lower-order accuracy than event-driven schemes, as they do not detect events exactly and produce incorrect gradient information at discontinuities.

An alternative approach involves smoothing techniques, which approximate the discontinuous right-hand side of the dynamics by using a smooth function. This method allows for simpler implementation and can be particularly useful for generating initial guesses in optimal control. Nonetheless, achieving accurate results with smoothing techniques requires a sufficiently small step size relative to the smoothing parameter which proves to be difficult in practice [24].

### B. Time-freezing approach for systems with state jumps

In the numerical results presented in this paper, we utilize the time-freezing approach for systems with state jumps, as introduced by [14]. This approach converts a system with state jumps into a Filippov differential inclusion by emulating the state jump within the infeasible region of the system. The resulting formulation ensures that discontinuities are present only in the right-hand side of the dynamics, while the state trajectories remain smooth. To this end, an auxiliary dynamical system  $f_{\text{aux}}(x)$  is defined in the infeasible region, where the trajectory endpoints adhere to the impact law while the progression of time is effectively frozen. We outline the main steps of the time-freezing approach in the following.

Consider system (1) with state vector  $x = (q, \dot{q})$ , impact surface  $f_c(q)$ , and input  $u$ . For  $f_c(q) > 0$  the reduced dynamics are given as  $\dot{x} = f_{\text{free}}(x, u)$ . One introduces a parameter for the numerical time  $\tau$  to define a clock state  $t(\tau)$  that stops evolving whenever  $f_{\text{aux}}(x)$  is active. This allows to differentiate between the numerical time  $\tau$  and the physical time  $t$  in the time-freezing system. To incorporate time evolution into our dynamics, one extends the state vector to  $\hat{x}(\tau) := (x(\tau), t(\tau)) \in \mathbb{R}^{n_x+1}$ . Time derivatives of the extended state vector with respect to the numerical time are compactly denoted as  $\hat{x}'(\tau) := \frac{d}{d\tau} \hat{x}(\tau)$ .

Next, one extends the impact surface using its time derivative to define the switching function  $c(\hat{x}) = (c_1(\hat{x}), c_2(\hat{x})) = (f_c(\hat{x}), \frac{d}{dt} f_c(\hat{x}))$  and specify the following regions

$$\begin{aligned} R_1 &= \{ \hat{x} \in \mathbb{R}^{n_x+1} \mid c_1(\hat{x}) > 0 \} \cup \{ \hat{x} \mid c_1(\hat{x}) < 0, c_2(\hat{x}) > 0 \}, \\ R_2 &= \{ \hat{x} \mid c_1(\hat{x}) < 0, c_2(\hat{x}) < 0 \}. \end{aligned} \quad (3)$$

Considering these regions and the extended state vector, the dynamics in region  $R_1$  are described by  $\hat{x}' = \hat{f}_{\text{free}}(\hat{x}, u) = (f_{\text{free}}(x, u), 1)$ , while the auxiliary dynamics in region  $R_2$  are given by  $\hat{x}' = \hat{f}_{\text{aux}}(\hat{x}) = (f_{\text{aux}}(x), 0)$ . Note that the control input  $u$  does not influence the system in  $f_{\text{aux}}(x)$ . The state and input trajectory for the original problem can be recovered by considering only the segments where  $\hat{x} \in R_1$ .

Finally, one can state the time-freezing system as

$$\begin{aligned} \hat{x}' \in F_{\text{TF}}(\hat{x}, u) &= \left\{ \theta_1 \hat{f}_{\text{free}}(\hat{x}, u) + \theta_2 \hat{f}_{\text{aux}}(\hat{x}) \mid \right. \\ &\left. \theta_1 + \theta_2 = 1, \theta_i \geq 0, \theta_i = 0 \text{ if } \hat{x} \notin \bar{R}_i, \forall i \in \{1, 2\} \right\}. \end{aligned} \quad (4)$$

For the simulation results in Section V we define such systems using the benchmarks introduced in Section IV.

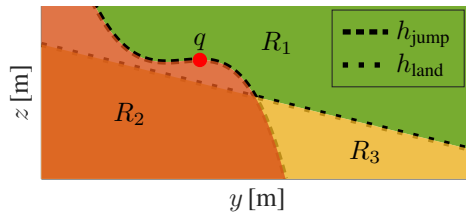


Fig. 1: Model of a ski jumping venue.

## IV. TWO TUTORIAL PROBLEMS

In the following, we present two tutorial problems that may also serve as benchmarks for nonsmooth dynamics and optimal control. The first problem concerns a ski jump scenario where the system model does not include any control inputs. Thus, we only focus on the numerical integration of the dynamics subject to state jumps and sliding modes. The second example is an OCP for bicycle dynamics navigating an uneven mountain bike track, with the objective of reaching a target location as quickly as possible without pedaling. The control input in this scenario is the reciprocal motion between the rider and the bicycle, referred to as *pumping*, which is the sole means of acceleration [15]. As discussed in the previous section, we employ the time-freezing approach for our simulations to model the impact behavior of the systems. To this end, we derive  $f_{\text{free}}(x, u)$  as well as the impact surfaces  $f_c(q)$  for both systems.

### A. Ski jump

We consider a ski jump as an example of a system exhibiting impacts and sliding motion. The system comprises a skier who jumps off a *take-off table* and lands on a *landing slope* with no control inputs. Simulations of this system allow us to examine how the starting height affects the point of impact, i.e., the distance covered by the jump.

The skier is modeled as a point mass with position  $q = (y, z) = (q_1, q_2) \in \mathbb{R}^2$  and velocity vector  $\dot{q}$ . The state of the system is  $x = (q, \dot{q}) \in \mathbb{R}^4$ . A sketch of the system is shown in Figure 1. Consequently, the system dynamics during free flight are given by

$$\dot{x} = f_{\text{free}}(x) = \left[ \dot{q}^\top, 0, -g \right]^\top \quad (5)$$

where  $g$  is the gravitational constant. We model the ski jump by considering the take-off table and the landing slope as  $h_{\text{jump}}(q_1)$  and  $h_{\text{land}}(q_1)$ . The impact surfaces from (1b), where the height of the skier  $q_2$  impacts the ground, are given by

$$f_{c1}(q) = q_2 - h_{\text{jump}}(q_1), \quad f_{c2}(q) = q_2 - h_{\text{land}}(q_1). \quad (6)$$

All impacts are assumed to be perfectly inelastic. Using these impact surfaces we define the following three regions:

$$\begin{aligned} R_1 &= \{ x \in \mathbb{R}^4 \mid f_{c1}(q_1) > 0 \wedge f_{c2}(q_1) > 0 \}, \\ R_2 &= \{ x \in \mathbb{R}^4 \mid f_{c1}(q_1) < 0 \}, \\ R_3 &= \{ x \in \mathbb{R}^4 \mid f_{c2}(q_1) < 0 \}. \end{aligned}$$

One can identify two operating modes: the free flight within

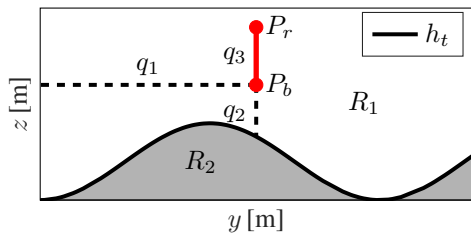


Fig. 2: Bicycle model on a pump track.

the interior of  $R_1$  and the sliding motion on the boundary defined by

$$\partial(R_1, R_2 \cup R_3) = \{x \in \mathbb{R}^4 \mid x \in \partial \overline{R_1} \cap x \in \partial \overline{R_2 \cup R_3}\}.$$

This boundary lies on the intersection of  $\partial \overline{R_1}$  and the closure of  $\partial \overline{R_2 \cup R_3}$ , encompassing their boundaries and limit points. Note that the infeasible region is in the interior of  $R_2 \cup R_3$ , and the system should not be initialized in this region.

### B. Accelerating a bike without pedaling

In this section, we formulate an OCP where a bicycle rider aims to reach a goal as quickly as possible without pedaling. Consider a bicycle and its rider on an uneven mountain bike track, also known as a pump track. As it is common knowledge in competitive cycling (in particular in BMX riding and mountain biking), riders can accelerate by strategically shifting their center of mass in response to the track's slope. Initial investigations as well as experimental results of this problem can be found in [15]. In this work, we extend these investigations by incorporating jumps that introduce nonsmoothness into the system. Similar to our previous work, we use a two-mass model connected by a mass-less link as bicycle-rider model. Figure 2 shows a sketch of the system. The generalized coordinates  $q = (q_1, q_2, q_3)$  are sufficient to describe the center of masses of bike and rider with masses  $m_b$  and  $m_r$ , respectively. The positions in the  $y$ - $z$ -plane are

$$P_b = \begin{bmatrix} q_1 \\ h_t(q_1) + q_2 \end{bmatrix}, \quad P_r = \begin{bmatrix} q_1 \\ h_t(q_1) + q_2 + q_3 \end{bmatrix},$$

where  $q_1$  corresponds to their  $y$ -coordinate,  $q_2$  is the slack above the ground, and the length of their connection is given by  $q_3$ . The height of the track is given as a nonlinear, differentiable function  $h_t(q_1)$ . For compact notation we denote its derivatives with respect to  $q_1$  as

$$h'_t = \frac{dh_t}{dq_1}, \quad h''_t = \frac{d^2h_t}{dq_1^2}.$$

The state vector is given by  $x = (q, \dot{q}) \in \mathbb{R}^6$ . We define our control input  $u$  as the exogenous force acting on  $q_3$ , which causes the reciprocal motion between both masses.

Using the Lagrangian formalism with generalized coordinates  $q(t)$ , we derive the reduced dynamics as

$$f_{\text{free}}(x, u) = \begin{bmatrix} \dot{q} \\ 0 \\ -(m_1 \dot{q}_1^2 h''_t + u + gm_1)/(m_1) \\ u(m_1 + m_2)/(m_1 m_2) \end{bmatrix} \in \mathbb{R}^6. \quad (7)$$

Similar to the ski jump, we consider the impacts to be perfectly inelastic. In this case, since we use a slack variable describing the height above the track, the impact surface from (1b) is trivially given by  $f_c = q_2$ . We define the regions

$$R_1 = \{x \in \mathbb{R}^6 \mid q_2 > 0\}, \quad R_2 = \{x \in \mathbb{R}^6 \mid q_2 < 0\}$$

to distinguish the operating modes of the system. In particular, the free motion in the interior of  $R_1$  and the sliding motion on the boundary between  $R_1$  and  $R_2$ , which will be addressed by extending to a time-freezing system (4) in Section V. The infeasible region is in the interior of  $R_2$ .

The goal is to reach a target location as quickly as possible using only pumping motion, leading to the following nonsmooth time-optimal control problem:

$$\min_{u(\cdot), t_f} t_f \quad (8a)$$

subject to for almost all  $t \in [0, t_f]$

$$(1), \quad x(0) = x_0 \quad (8b)$$

$$l_{\min} \leq q_3 \leq l_{\max}, \quad u_{\min} \leq u \leq u_{\max} \quad (8c)$$

$$q_1(t_f) = q_{\text{goal}}, \quad (8d)$$

where,  $t_f$  is the free terminal time,  $x_0$  is the initial condition, and (8d) is the terminal constraint. To impose realistic state and input constraints (8c), experimental results were reported in [15]. Specifically, during test rides on a real pump track, the centers of mass of the bicycle and the rider were captured separately using a 3D camera system. This data is utilized to analyze the distance  $l = q_3$  between the two masses, as well as the corresponding acceleration  $\ddot{q}_3$ . This led to the boundaries of the state constraint  $\mathbb{X} = \{x \mid l_{\min} \leq q_3 \leq l_{\max}\}$ . Using the relation  $\ddot{q}_3 = u(m_1 + m_2)/(m_1 m_2)$  from (7), we can determine the input constraint  $\mathbb{U} = \{u \mid u_{\min} \leq u \leq u_{\max}\}$  based on the measurements of  $\ddot{q}_3$ .

### C. Scalability of the proposed problems

In its current form, the ski jump model serves as a testbed solely for simulating nonsmooth dynamics. However, it can be easily extended to be used for optimal control. One straightforward extension, requiring no additional modeling effort from the user, is to include the skier's initial velocity as a decision variable in the OCP. This can be interpreted as the impulse generated when the athlete pushes off the starting bench to accelerate. Alternatively, or in addition, the model can be extended to include a control action at the take-off table. Given the significance of air drag in ski jumping, incorporating it into the model would provide valuable insights into its impact on performance.

Similarly, the complexity of the pump track problem can be scaled to challenge numerical methods. For instance, the bicycle model can be extended to include two ground-contact points, resulting in simultaneous impacts that must be handled by the numerical approach. The total number of impacts can be varied by adjusting the initial velocity, simulation time, or characteristics of the impact surface. Additionally, more complex impact surfaces could be considered, such as a discontinuous surface to model the bicycle jumping over a gap,

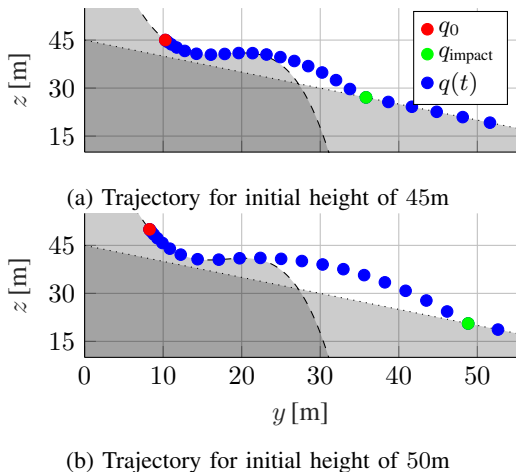


Fig. 3: Ski jumping – results for two different initial heights.

or a series of impact surfaces to represent a complete track. Finally, modeling ground contact using Coulomb friction would impose a second type of nonsmoothness.

## V. SIMULATION RESULTS

Implementations of the examples and MATLAB simulation code are publicly available at [<https://github.com/OptCon/PumpTrackOC>]. This repository includes the implementation of both examples using *nosnoc* [9] and *CasADi* [29]. We employ the finite element with switch detection method [30], an event-driven integration scheme.

*Ski jump*: For the ski jump example, we use the automatic model reformulation provided by *nosnoc*. Here, we provide the mass matrix, which is trivial in the case of a single point mass, the reduced dynamics (5), and the impact surfaces (6). Simulation results are shown in Figure 3. The figure depicts the trajectories with the starting and impact position highlighted. As anticipated, increasing the initial height shifts the point of impact further to the right. While these results are predictable, the simplicity of the problem is precisely what makes it well-suited for prototyping and testing new solution approaches. The complexity, in its current form, stems primarily from handling nonlinear impact surfaces.

*Bicycle pumping*: As discussed in Section III-B, applying the time-freezing approach to the pump track problem involves the design of auxiliary dynamics to simulate the impact behavior in its infeasible region while freezing physical time. For the extended state  $\hat{x}(\tau) = (x(\tau), t(\tau)) \in \mathbb{R}^7$ , we define the auxiliary dynamics as

$$\hat{f}_{\text{aux}}(\hat{x}) = k_n \begin{bmatrix} 0, 0, 0, -h'_t(q_1), 1, 0, 0 \end{bmatrix}^\top \in \mathbb{R}^7$$

with  $k_n > 0$ . By extending the reduced dynamics to the augmented state, we obtain  $\hat{f}_{\text{free}}(\hat{x}, u) = (f_{\text{free}}(x, u), 1)$ , which incorporates the additional time dimension. Using this formulation, and the regions  $R_1$  and  $R_2$  from (3), we obtain the time-freezing system (4).

Figure 4 shows the simulation results for the pump track system. It compares the trajectories of the system for different

initial velocities  $v_{1,0} = \dot{q}_{1,0}$  without input and with the optimal input  $u^*$  to problem (8). The results without input in Figures 4a–4c show three different scenarios depending on the initial velocity. From left to right: (i) not reaching  $q_{\text{goal}}$ , (ii) reaching  $q_{\text{goal}}$  while maintaining ground contact, and (iii) reaching  $q_{\text{goal}}$  with a jump. From a rider’s perspective, scenario (iii) represents a jump landing, which should be avoided because the impact with the incline significantly reduces speed. The optimal solutions in Figures 4d–4f show the trajectories for the same initial velocities with the optimal input  $u^*$ . We can see, for scenario (i), the optimal input accelerates the system to successfully reach the goal. For scenario (iii), the optimal input avoids jumping and hitting the landing slope while still reaching the goal. To analyze the velocities and times for each scenario, we show the solution trajectories in Figure 5. In scenario (ii), we observe the highest velocity gain through pumping, with  $\Delta v_1 = 7.56$  km/h, as shown in Figure 5b. The time required to reach the goal is decreased from 1.87 s to 1.42 s, see Figure 5a. Figures 5c and 5d show the trajectories of  $q_3(\cdot)$  and  $u^*(\cdot)$ , satisfying the state and input constraints.

## VI. CONCLUSION

This paper has proposed two novel problems for simulation and optimal control of nonsmooth dynamics: a basic ski jumping model and optimal control of a bicycle on a pump track. Due to the fact that the underlying physics in both examples are straightforward to understand, these problems have potential for teaching purposes. Additionally, the scalability of the bicycle problem makes it potentially useful for comparing and evaluating state-of-the-art methods in numerical nonsmooth optimal control.

Simulation results using a time-freezing approach for treating the state jumps of the systems have been presented. The solutions of the pump track model, which extend on the initial investigations in [15] by incorporating jumps, closely match real-world observations on mountain bike tracks. Future work will extend to a multi-body system with two tires and incorporate friction.

## REFERENCES

- [1] A. J. Van Der Schaft and H. Schumacher. *An Introduction to Hybrid Dynamical Systems*, volume 251. Springer, 2007.
- [2] R. I. Leine and N. Van de Wouw. *Stability and Convergence of Mechanical Systems with Unilateral Constraints*, volume 36. Springer Science & Business Media, 2007.
- [3] V. Acary and B. Brogliato. *Numerical Methods for Nonsmooth Dynamical Systems: Applications in Mechanics and Electronics*. Springer Science & Business Media, 2008.
- [4] S. Sager. A benchmark library of mixed-integer optimal control problems. In *Mixed Integer Nonlinear Programming*, pages 631–670. Springer, 2011.
- [5] L. F. S. Larsen, R. Izadi-Zamanabadi, R. Wisniewski, and C. Sonntag. Supermarket refrigeration systems—a benchmark for the optimal control of hybrid systems. *Technical report for the HYCON NoE*, 2007.
- [6] M. Alamir. A benchmark for optimal control problem solvers for hybrid nonlinear systems. *Automatica*, 42(9):1593–1598, 2006.
- [7] C. Seatzu, D. Corona, A. Giua, and A. Bemporad. Optimal control of continuous-time switched affine systems. *IEEE Transactions on Automatic Control*, 51(5):726–741, 2006.
- [8] C. Kirches, E. Kostina, A. Meyer, and M. Schlöder. Numerical solution of optimal control problems with switches, switching costs and jumps. *Optimization Online*, 6888(205):1–30, 2018.



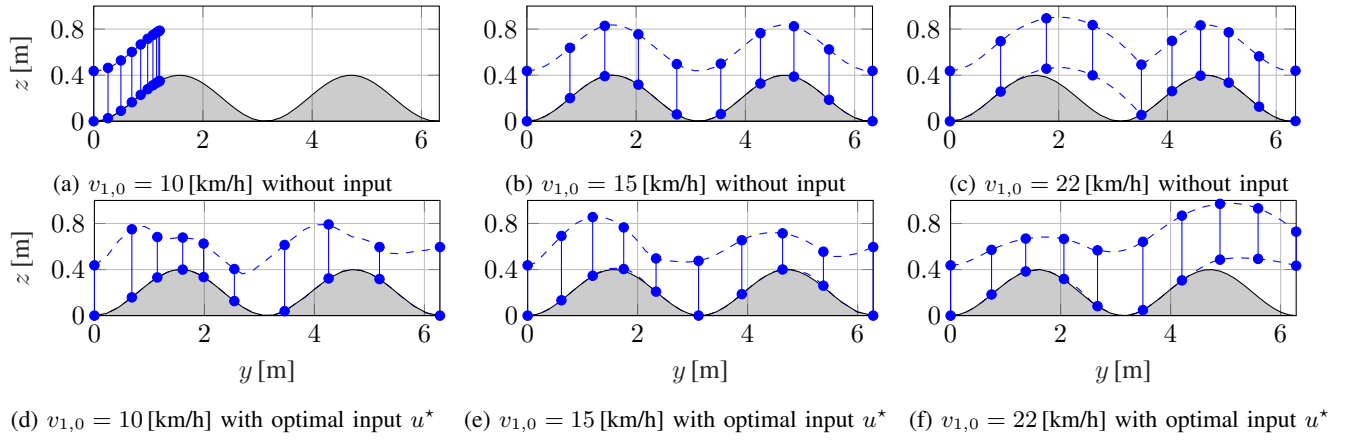


Fig. 4: Bicycle on pump track – simulation results for three different scenarios. The first row shows the system without input, and the second row shows the system with the optimal input  $u^*$ .

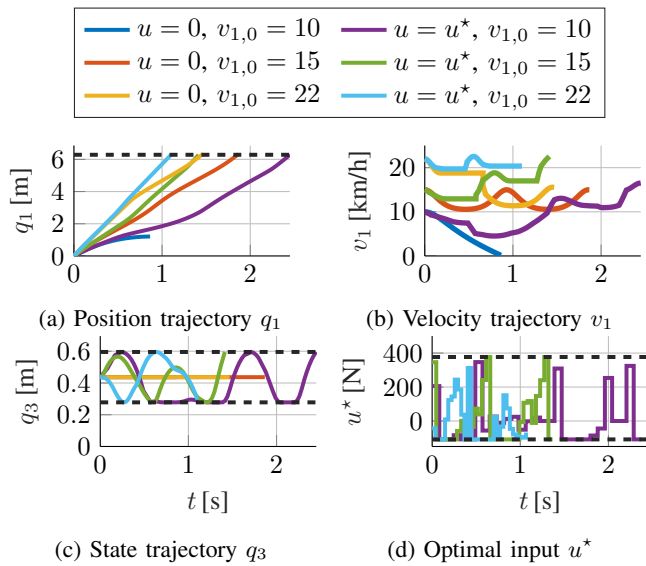


Fig. 5: Bicycle on pump track – solution trajectories over time. The optimal input  $u^*$ , the pumping motion, accelerates the system to reach the goal faster and to gain velocity.

[9] A. Nurkanović and M. Diehl. Noscoc: A software package for numerical optimal control of nonsmooth systems. *IEEE Control Systems Letters*, 6:3110–3115, 2022.

[10] I. M. Ross and F. Fahroo. A direct method for solving nonsmooth optimal control problems. *IFAC Proceedings Volumes*, 35(1):479–484, 2002.

[11] A. Nurkanović, A. Pozharskiy, and M. Diehl. Solving mathematical programs with complementarity constraints arising in nonsmooth optimal control. *Vietnam Journal of Mathematics*, pages 1–39, 2024.

[12] K. J. Åström and J. Lunze. Warum können wir fahrrad fahren? *at Automatisierungstechnik* 49, 2001.

[13] K. J. Åström, R. E. Klein, and A. Lennartsson. Bicycle dynamics and control: adapted bicycles for education and research. *IEEE Control Systems*, 25(4):26–47, aug 2005.

[14] A. Nurkanović, S. Albrecht, B. Brogliato, and M. Diehl. The time-freezing reformulation for numerical optimal control of complementarity lagrangian systems with state jumps. *Automatica*, 158:111295, 2023.

[15] J. Golembiewski, M. Schmidt, B. Terschluse, T. Jaitner, T. Liebig, and T. Faulwasser. The dynamics of a bicycle on a pump track—first results on modeling and optimal control. *at-Automatisierungstechnik*,

72(2):134–142, 2024.

[16] M. Bernardo, C. Budd, A. R. Champneys, and P. Kowalczyk. *Piecewise-Smooth Dynamical Systems: Theory and Applications*, volume 163. Springer Science & Business Media, 2008.

[17] D. Liberzon. *Switching in Systems and Control*, volume 190. Springer, 2003.

[18] A. F. Filippov. *Differential Equations with Discontinuous Righthand Sides: Control Systems*, volume 18. Springer Science & Business Media, 2013.

[19] W. P. M. H. Heemels and B. Brogliato. The complementarity class of hybrid dynamical systems. *European Journal of Control*, 9(2-3):322–360, 2003.

[20] B. Brogliato and A. Tanwani. Dynamical systems coupled with monotone set-valued operators: Formalisms, applications, well-posedness, and stability. *Siam Review*, 62(1):3–129, 2020.

[21] T. Westenbroek, X. Xiong, A. D. Ames, and S. Shankar Sastry. Optimal control of piecewise-smooth control systems via singular perturbations. In *2019 IEEE 58th Conference on Decision and Control (CDC)*, pages 3046–3053, 2019.

[22] G. Colombo, R. Henrion, D. H. Nguyen, and B. S. Mordukhovich. Optimal control of the sweeping process over polyhedral controlled sets. *Journal of Differential Equations*, 260(4):3397–3447, 2016.

[23] A. Vieira, B. Brogliato, and C. Prieur. Quadratic optimal control of linear complementarity systems: First-order necessary conditions and numerical analysis. *IEEE Transactions on Automatic Control*, 65(6):2743–2750, 2020.

[24] A. Nurkanović. *Numerical Methods for Optimal Control of Nonsmooth Dynamical Systems*. PhD thesis, Universität Freiburg, 2023.

[25] Y. Kim, S. Leyffer, and T. Munson. MPEC methods for bilevel optimization problems. *Bilevel Optimization: Advances and Next Challenges*, pages 335–360, 2020.

[26] M. Diehl, H. G. Bock, H. Diedam, and P.-B. Wieber. Fast direct multiple shooting algorithms for optimal robot control. *Fast motions in biomechanics and robotics: optimization and feedback control*, pages 65–93, 2006.

[27] B. Brogliato. *Nonsmooth Mechanics: Models, Dynamics and Control*. Springer, 3rd edition, 2016.

[28] D. E. Stewart and M. Anitescu. Optimal control of systems with discontinuous differential equations. *Numerische Mathematik*, 114:653–695, 2010.

[29] J. A. E. Andersson, J. Gillis, G. Horn, J. B. Rawlings, and M. Diehl. Casadi: a software framework for nonlinear optimization and optimal control. *Mathematical Programming Computation*, 11:1–36, 2019.

[30] A. Nurkanović, M. Sperl, S. Albrecht, and M. Diehl. Finite elements with switch detection for direct optimal control of nonsmooth systems. *Numerische Mathematik*, pages 1–48, 2024.